siRNA. Approximately 80 pmol siRNA were delivered to 1×10^5 cells. The cell culture medium was removed, and the HVJ envelope vector was added to each well. Thirty minutes later, the medium containing the vector was replaced with fresh medium.

Western blot analysis

The harvested human cancer cells were lysed in lysis buffer (1% SDS, 20 mM Tris-HCl (pH 8), 135 mM NaCl, 10% glycerol, and a protease inhibitor mixture (Roche, Basel, Switzerland)). After adding 2× sample buffer (0.1 M Tris-HCl (pH 6.8), 4% SDS, 12% 2-mercaptoethanol, 20% glycerol, and 0.01% bromphenol blue), 30 μg of protein were separated by 10% sodium dodecyl sulfate/polyacrylamide gel electrophoresis (SDS-PAGE) and transferred onto a polyvinylidene fluoride membrane (Millipore, Bedford, MA, USA). The membrane was blocked with 5% skim milk and subsequently probed with antibodies, anti-human Rad51 (Santa Cruz, Santa Cruz, CA, USA), anti-β-actin (Abcam, Cambrige, UK), and anti-GAPDH (Ambion, Austin, TX, USA). Proteins were detected with horseradish peroxidase labeled anti-goat (Santa Cruz) or anti-mouse (Amersham, Piscataway, NJ, USA) antibodies and the enhanced chemiluminescence reagent (Amersham).

Northern blot analysis

Total RNA was isolated from HeLa cells using ISOGEN (Nippon Gene, Toyama, Japan) according to the manufacturer's instructions. Total RNA (15 μg/lane) was separated in a formaldehyde/1.5% agarose gel, transferred to Hybond N+ membrane (Amersham), and then hybridized with ^{32}P-labeled Rad51 and G3PDH cDNA probes.

Colony forming assay

Twenty-four hours after HVJ envelope vector-mediated siRNA transfection to HeLa cells *in vitro*, the cells were seeded in a 6-cm dish at a density of 10^3 cells/dish and treated with 0–0.1 μg/ml CDDP for 3 h. After 7 days, the colonies were fixed with methanol and stained with Giemsa (Nacalai Tesque). Then, the colonies were counted. The percentage of colony-forming cells after CDDP treatment was calculated and compared to the untreated control group.

CDDP sensitivity in cultured cells by Rad51 siRNA transfer

Forty-eight hours after transfer of siRNA, the cells were treated with 0.1, 0.3 and 1.0 μg/ml CDDP for 3 h. Then, 48 h later, cell number was counted using a particle counter (Coulter Corporation, Miami, FL, USA). To assess apoptosis, cells treated with Rad51 siRNA and CDDP were harvested and stained with fluorescent isothiocyanate-labeled Annexin V (Becton Dickinson, San Diego, CA, USA) for 20 min at room temperature. The labeled cells were analyzed with FACScan (Becton Dickinson).

In vivo experiments

Viable HeLa cells (5×10^6 cells) were resuspended in 100 μl of PBS and intradermally injected into the right flanks of 6-week-old male SCID mice (Charles River Japan, Yokohama, Japan). The inactivated HVJ suspension (6×10^9 particles) was mixed with 60 μl of 250 μM Rad51 siRNA solution and 6 μl of 2% Triton X-100. Scrambled siRNA solution was used as a control. After centrifugation (18 500 *g*, 15 min) at 4 °C, the supernatant was removed and the HVJ envelope vector containing siRNA was suspended in 120 μl of PBS. Seven days after tumor inoculation, 100 μl (5×10^9 particles) of HVJ envelope vector containing siRNA were injected into the tumor. Approximately 2.5 nmol siRNA were delivered to the tumor mass in a mouse. The injection

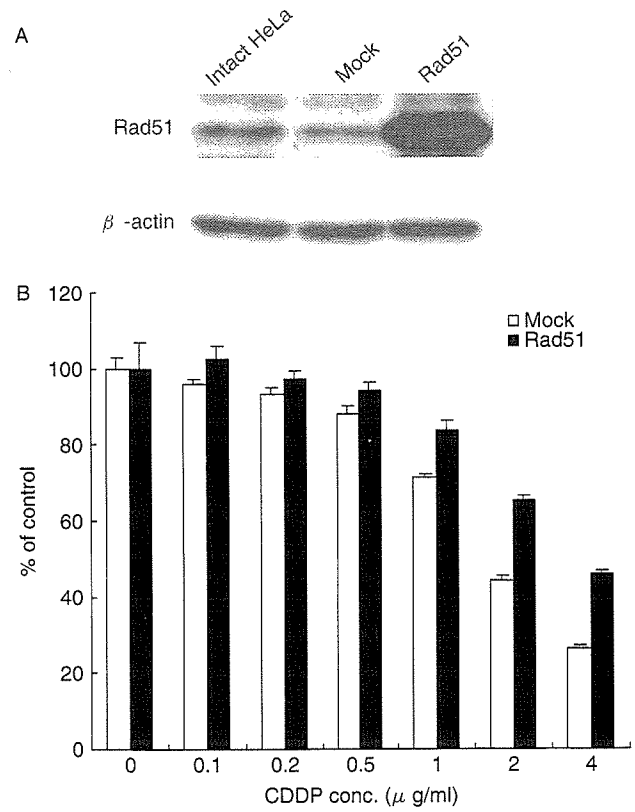

Figure 1. (A) Detection of human Rad51 transcript 48 h after the transfection of human Rad51 cDNA driven by the CMV promoter. Mock sample indicates HeLa cells transfected with a plasmid that did not contain Rad51 cDNA. Intact HeLa indicates HeLa cells that were not transfected. (B) Cell survival was detected by a modified MTT assay after treatment with 0–4 μg/ml CDDP for 3 h. The ordinate indicates the ratio of viable cells treated with various concentrations of CDDP to initial cell number. The mean value ± standard deviation from triplicate samples is shown

was repeated at 2-day intervals until each mouse received a total of three injections. At the time of the second siRNA injection, 200 μg of CDDP were intraperitoneally injected. Tumor size was measured every 2 days, and the tumor volume was calculated using the simplified formula for a rotational ellipse ($l \times w^2 \times 0.5$). All animals were treated in a humane fashion in accordance with the guidelines of the Animal Committee of Osaka University.

Results

To determine what factors induced by CDDP contribute to the repair of DNA damage, we examined the gene expression of repair genes in cells treated with CDDP. The protein level of Rad51, which is involved in homologous recombination repair, increased 1.57 ± 0.4 times more with CDDP than that without CDDP (data not shown). However, the expression level of Ku70, which is involved in non-homologous end joining, was not changed (0.9 ± 0.3 times) by CDDP treatment.

We examined whether Rad51 expression resulted in resistance to CDDP. To increase the expression of Rad51, HeLa cells were transfected with the human Rad51 gene driven by the cytomegalovirus (CMV) promoter (Figure 1A). When cell proliferation was measured by a modified MTT assay, Rad51-transfected HeLa cells cultured with various concentrations of CDDP were more viable than control cells that had undergone only a mock transfection (Figure 1B). The experiment was repeated three times, and similar results were obtained.

To enhance sensitivity to CDDP, we attempted to suppress Rad51 expression with siRNA. When Cy3-labeled siRNA was delivered to HeLa cells using the HVJ envelope vector, the efficiency was 80–100% (data not shown). Rad51 transcripts were not detected by Northern blot analysis 1 day after siRNA delivery, whereas scrambled siRNA did not reduce the transcript level (Figure 2A). We tested five different siRNAs for Rad51, but the only effective siRNA was a 19-mer from no. 321 of the Rad51 mRNA sequence. The other four siRNAs (19-mers from nos. 89, 462, 828, and 989) did not suppress Rad51 expression (data not shown). Two different antisense oligonucleotides against human Rad51 did not reduce the expression of human Rad51 (Figure 2B). These oligonucleotides had the same sequence as mouse Rad51 antisense oligonucleotides that had been used for suppression of Rad51 [32]. Rad51 protein was not detected by Western blots for 4 days after siRNA transfer. A small amount of Rad51 protein began to reappear on day 5 (Figure 2C). When Rad51 siRNA was introduced into HeLa cells, the growth of the cells was suppressed and the viability was 70% less than cells treated with scrambled siRNA (Figure 3A). The growth of cells treated with scrambled siRNA was not significantly different compared to that of cells treated with HVJ-E containing PBS. When HeLa cells were incubated with 0.02 μg/ml CDDP for 3 h after the delivery of Rad51 siRNA, the survival of the cells was reduced by 90% when compared to equivalent cells that were not exposed to CDDP (Figure 3B). More than 90% of colonies were formed with the same concentration of CDDP when scrambled siRNA was transferred into HeLa cells. Accordingly, with Rad51

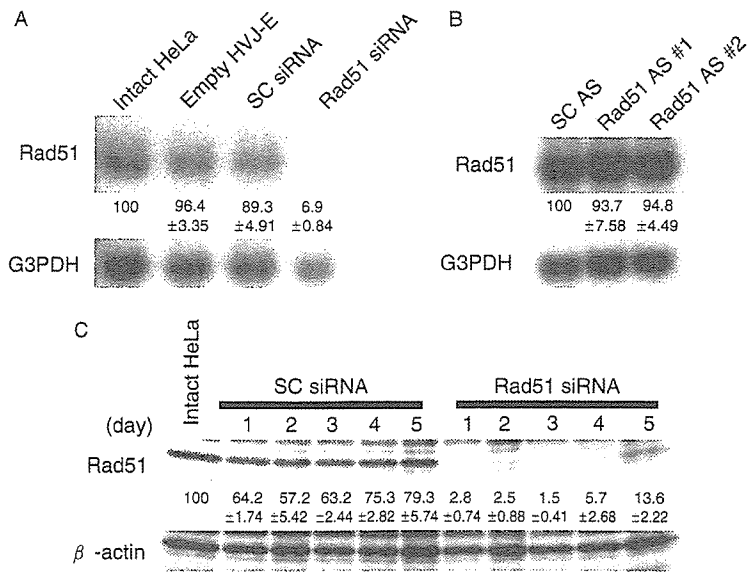

Figure 2. (A) Rad51 transcripts detected by Northern blot analysis 1 day after the delivery of Rad51 siRNA or scrambled (SC) siRNA. Rad51 mRNA in intact HeLa cells and HeLa cells treated with empty HVJ envelope vector were also measured. (B) Rad51 detection by Northern blot analysis 1 day after the delivery of two different antisense oligonucleotides (#1 and #2) against human Rad51 (Rad51 AS) or scrambled oligonucleotides (SC AS). (C) Rad51 protein detected by Western blot on days 1 to 5 after the delivery of either Rad51 siRNA or SC siRNA. These experiments were repeated twice and similar results were obtained. The ratio of Rad51 expression to G3PDH or β-actin expression was calculated by measuring the density of each band using the NIH imager. The percentage of Rad51 expression (mean ± standard deviation) is shown below each lane

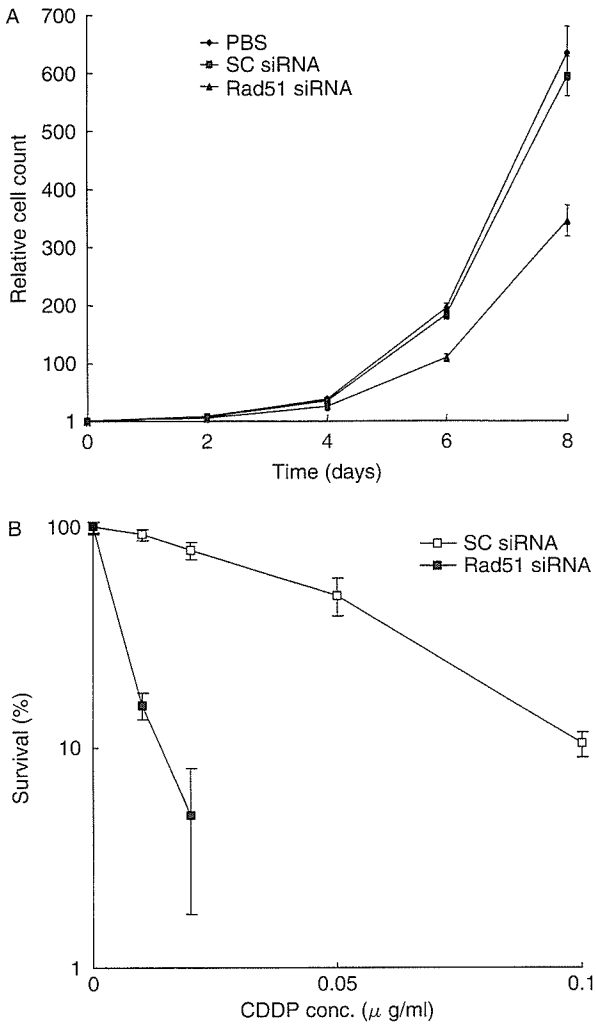

Figure 3. (A) The growth of HeLa cells detected by cell count on days 0 to 8 after the delivery of Rad51 siRNA, scrambled (SC) siRNA or PBS using the HVJ envelope vector. (B) The colony formation of HeLa cells after the delivery of either Rad51 siRNA or SC siRNA. The ordinate indicates the ratio of the number of colonies in the presence of various concentrations of CDDP to the number of colonies without CDDP after the delivery of siRNA. The mean value ± standard deviation from triplicate samples is shown at each point of both experiments. No colonies were observed at 0.05 and 0.1 μg/ml CDDP when Rad51 siRNA was delivered

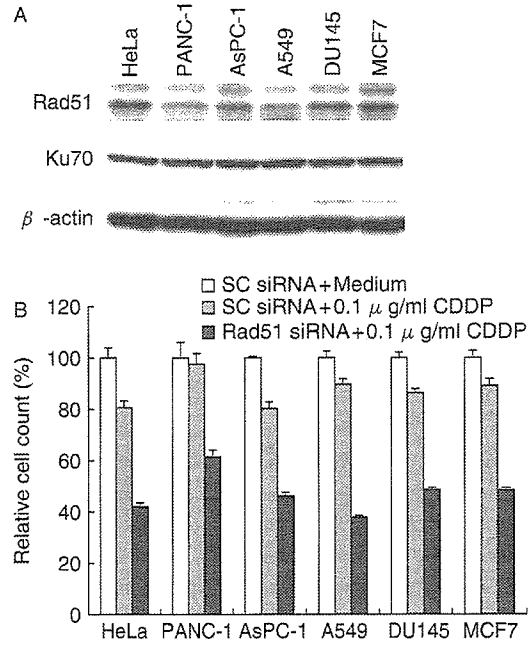

Figure 4. The increase in CDDP sensitivity in various cancer cell lines with Rad51 siRNA. (A) Rad51 and Ku70 protein levels in various cancer cell lines were detected by Western blotting. (B) siRNA was introduced into the human cancer cells using the HVJ envelope vector on day 1 after the inoculation of 10^5 cells in a 6-well plate. On day 3, cells were incubated with CDDP (0.1 μg/ml) for 3 h, and cell number was counted using a particle counter on day 5. Relative cell count indicates the ratio of cell number (the mean value of triplicate samples) treated with either scrambled (SC) or Rad51 siRNA + CDDP to that treated with SC siRNA + medium

siRNA, the number of colonies decreased to approximately 10% of that with scrambled siRNA.

We tested the effect of Rad51 siRNA on the sensitivity of CDDP in various human cancer cell lines including PANC-1 (pancreatic cancer), AsPC-1 (pancreatic cancer), A549 (lung cancer), DU145 (prostate cancer), MCF7 (mammary carcinoma), and HeLa S-3 (cervical cancer). First, the amounts of Rad51 and Ku70 in these human cancer cells were detected by Western blotting. The protein levels of Rad51 varied among cell lines while Ku70 protein levels were almost similar (Figure 4A). Then, on day 2 after the treatment with CDDP (0.1 μg/ml), the ratio of cell numbers of these cancer cell lines was examined in the presence of Rad51 siRNA or scrambled siRNA introduced using the HVJ envelope vector. Without Rad51 siRNA, more than 80% of the cells were still alive in all the cancer cell lines. Scrambled siRNA did not induce any toxicity in all the cell lines. However, with Rad51 siRNA, Rad51 protein level was reduced to less than 10% of that without siRNA in all the cell lines (data not shown), and all the cell lines were much more sensitive to CDDP. The sensitivity to CDDP increased more than 30% in all cases (Figure 4B). Thus, the enhancement of CDDP sensitivity by Rad51 siRNA appeared to be generally applicable to many cancer cells.

Next, we examined the sensitivity to CDDP in non-cancerous human cells after transfer of Rad51 siRNA. As shown in Figure 5A, the sensitivity to CDDP was not enhanced in NHDF when the concentration of CDDP increased. Then, we compared the apoptosis of NHDF to that of HeLa cells by the treatment with Rad51 siRNA in the presence or absence of 0.1 μg/ml CDDP (Figure 5B). The apoptotic cell ratio was not significantly different between HeLa cells (4.0 ± 1.1%) and NHDF (3.2 ± 0.5%) with Rad51 siRNA in the absence of CDDP. However, in the presence of CDDP, the apoptosis increased to 15.0% in HeLa cells, while it was 4.9% in NHDF.

We examined the ability of CDDP and Rad51 siRNA to suppress tumor growth in SCID mice. First, to test the gene delivery efficiency *in vivo*, we injected the HVJ

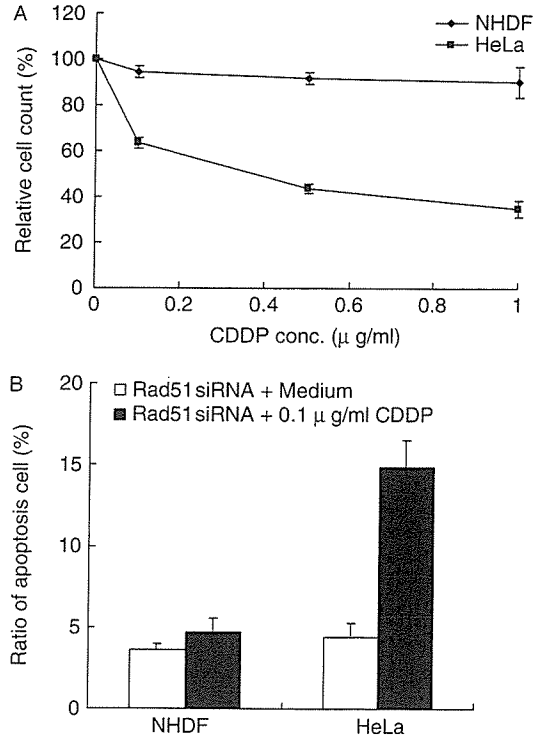

Figure 5. Rad51 siRNA did not enhance the sensitivity to CDDP in NHDF. (A) Forty-eight hours after transfer of Rad51 siRNA, the cells were treated with 0.1, 0.3 and 1.0 μg/ml CDDP for 3 h. Then, 48 h later, cell number was counted using a particle counter. Relative cell count indicates the ratio of cell number (the mean value of triplicate samples) treated with CDDP to that treated with medium alone. (B) To assess apoptosis, cells treated with Rad51 siRNA and CDDP were stained with fluorescein isothiocyanate (FITC)-labeled Annexin V and analyzed with FACScan. The ordinate indicates the ratio of labeled cells treated with Rad51 siRNA + medium or Rad51 + CDDP to that with scrambled siRNA + medium

envelope vector containing fluorescein isothiocyanate (FITC)-labeled oligodeoxynucleotides (FITC-ODN) into HeLa cell-derived tumors. As shown in Figure 6, the number of FITC-labeled cells and cells stained with Hoechst in randomly selected fields of three independent experiments were counted. They were 1227/2256, 616/1360, and 769/1424 cells. Thus, the delivery efficiency of FITC-ODN to HeLa cell tumors *in vivo* was 51.5 ± 5.2% (mean ± standard deviation). Next, Rad51 siRNA was delivered to tumors using the HVJ envelope vector. Western blot analysis showed that the level of Rad51 transcript was reduced to approximately 25% of that in intact HeLa tumors (Figure 7). Intraperitoneal injection of 200 μg of CDDP on day 2 transiently suppressed tumor growth, but tumors began to grow again 8 days after the treatment. To enhance the anti-tumor effect of CDDP, Rad51 siRNA delivered by the HVJ envelope vector was injected into the tumors on days 0 and 2. However, the suppression of tumor growth was not significant when compared to CDDP treatment alone (data not shown). Finally, Rad51 siRNA was injected into tumor mass on days 0, 2, and 4, and CDDP was injected into the abdominal cavity on day 2. This combination treatment significantly reduced the growth of HeLa tumors when compared to other treatment groups (Figure 8). Thus, the combination of CDDP and Rad51 siRNA is an effective anti-cancer protocol.

Discussion

We enhanced the sensitivity of cancer cells to CDDP by completely suppressing Rad51 with siRNA. The combination of CDDP and siRNA caused the regression of human tumors in mice. These results support the theory that DNA damage induced by CDDP can be repaired by Rad51. Our results suggest that CDDP-induced DNA damage can be repaired by homologous recombination of DNA double-strand breaks. We succeeded in suppression of Ku70 proteins in HeLa cells using Ku70 siRNA, but the sensitivity to CDDP was not enhanced in HeLa cells (data not shown). An antisense Ku70 study supports our observation [18]. Although we have not applied siRNA technology to suppress another factors such as Ku80 and DNA protein kinase (DNA-PK) which are also involved in non-homologous DNA end joining, it has been reported that silencing of DNA-PK or Ku86 by siRNA enhances sensitivity to radiation and anti-cancer drugs such as methyl methanesulfonate and bleomycin, but not to DNA cross-linking agents such as cisplatin and chlorambucyl [32–34]. Moreover, cisplatin killing is mediated by kinase activity of the Ku70, Ku80 and DNA-PK complex [35]. However, another report indicates that novel inhibitors of DNA-PK, vanillins, sensitize cells to cisplatin [36]. Thus, the involvement of DNA-PK in cisplatin sensitivity is still controversial. A comparative study of Rad51 siRNA and DNA-PK siRNA in cisplatin sensitivity should be conducted.

siRNA very effectively suppressed Rad51 expression. A previous study found that antisense oligodeoxynucleotides against mouse Rad51 enhanced the radiosensitivity of malignant glioma [37]. Although the target sequence of the antisense oligonucleotides is the same in humans and mice, the antisense oligonucleotides to human Rad51 did not suppress human Rad51 mRNA (Figure 2). As shown in Figure 2, Rad51 protein completely disappeared for 4 days after the siRNA transfer. We have never observed such complete loss of target protein using either antisense oligonucleotides or ribozymes. However, only one of five siRNA constructs effectively suppressed Rad51 expression. The system for predicting effective siRNA sequences should be improved.

When siRNA was delivered using the HVJ envelope vector, the efficiency was almost 100% in cultured cells, and Rad51 expression was completely prevented for 4 days after the delivery. siRNA very effectively suppresses gene expression, especially when an efficient delivery system is used. However, even when the HVJ envelope vector was used, the efficiency of a single siRNA injection into a tumor was only 50%. One limitation of synthetic siRNA is that its effect is transient, probably because

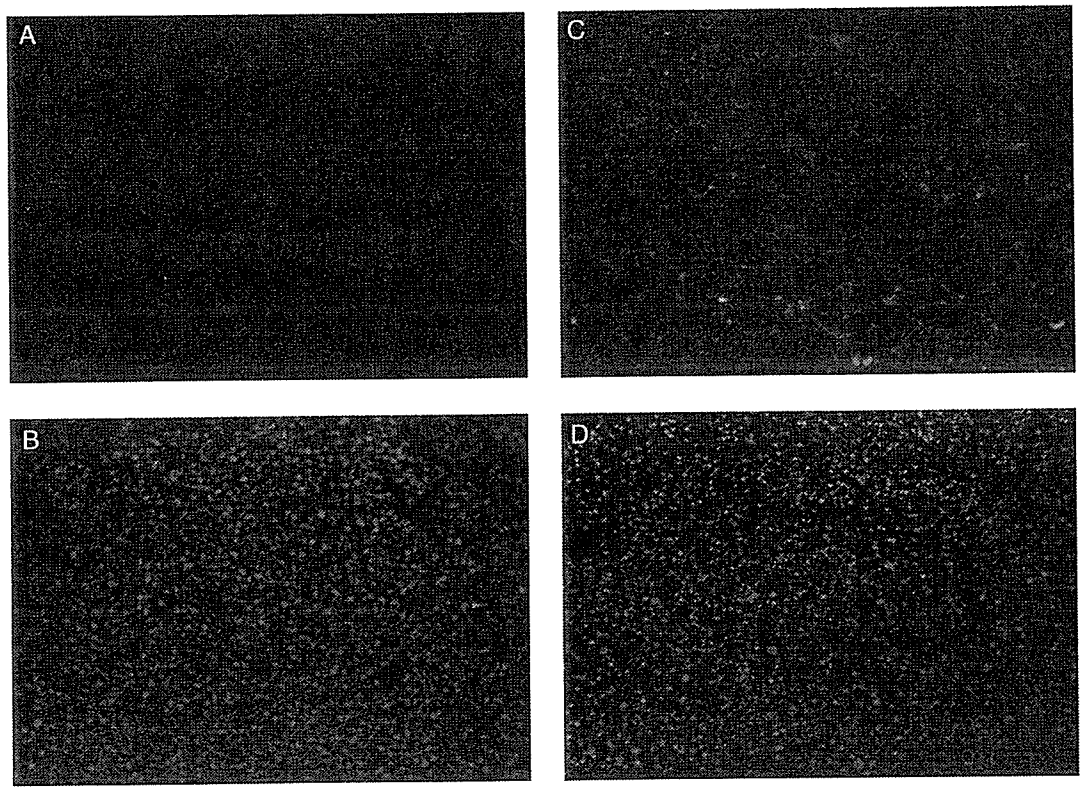

Figure 6. Detection of FITC-labeled ODN in tumors derived from HeLa cells in SCID mice. HVJ envelope vector containing unlabeled ODN (A, B) or FITC-ODN (C, D) was injected into tumors. FITC was detected in A and C. Hoechst 33 258 was used to counterstain the nucleus (B and D). The experiments were repeated three times and representative photos are shown

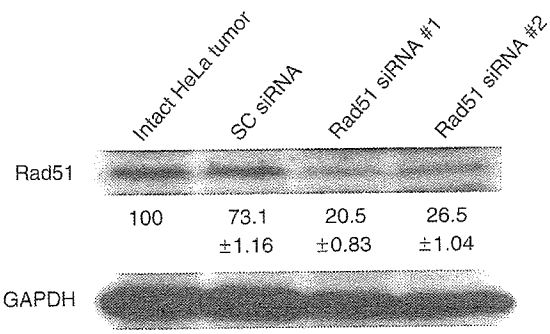

Figure 7. Rad51 transcript was detected by Western blot analysis after the delivery of either Rad51 siRNA or scrambled (SC) siRNA. The samples were isolated from two mice (#1 and #2) injected with the same Rad51 siRNA. This experiment was repeated twice and similar results were obtained. The percentage of Rad51 expression (mean ± standard deviation) below in each lane was calculated as described in Figure 2

the siRNA is gradually diluted after cell division. The use of lentivirus vector or retrovirus vector to insert siRNA expression DNA into the host chromosome has been proposed [38,39]. However, we believe that a combined treatment of synthetic siRNA and CDDP is sufficient for cancer treatment, because the cells that received Rad51 siRNA and CDDP in this study died in a few days. An important factor in the success of the combination treatment is the consecutive delivery of synthetic siRNA. Indeed, three injections of Rad51 siRNA into the tumor were more effective for tumor regression than two injections. The immunogenicity of the HVJ envelope vector is much less than that of native HVJ because of the inactivation of the viral genome. Consecutive injection is feasible with this vector system [28].

Rad51 siRNA enhanced the sensitivity to another anti-cancer drug, bleomycin, which can induce DNA double-strand breaks. The enhancement of bleomycin sensitivity by Rad51 siRNA was almost similar to that in a CDDP experiment (M. Ito and Y. Kaneda, unpublished data). It has been reported that Rad51 is also involved in the sensitivity of cancers to other anti-cancer drugs, such as etoposide (VP16) and imatinib mesylate (Gleevec) [40,41]. Since only Rad51 siRNA decreased cancer cell viability (Figure 4A), Rad51 siRNA can also enhance the sensitivity of cancer cells to other drugs which do not induce DNA double-strand breaks. This experiment is being performed in our laboratory. Furthermore, although Rad51 expression levels varied from cell line to cell line, all the cancer cells became very sensitive to CDDP in combination with Rad51 siRNA. The sensitivity of the cancer cell lines to CDDP did not appear to be related to the endogenous Rad51 protein level. These results suggest that the combination of CDDP with Rad51 siRNA will be generally applicable to various human cancers.

The enhancement of CDDP sensitivity by Rad51 siRNA was observed only in HeLa cells, not in NHDF. Similarly, apoptosis by Rad51 siRNA and CDDP increased in

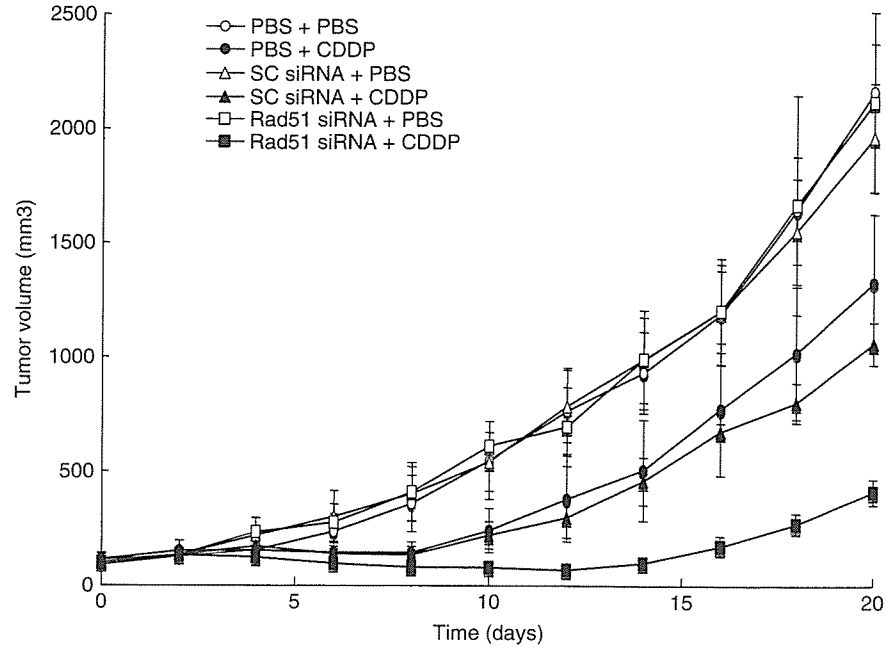

Figure 8. Tumor volume in SCID mice. Intraperitoneal injection of CDDP on day 2 transiently suppressed tumor growth *in vivo*, but tumors began to grow again 8 days after the treatment. To enhance the anti-tumor effect of CDDP, Rad51 siRNA or scrambled (SC) siRNA was injected on days 0, 2, and 4. In three groups, 200 μg of CDDP were injected into the abdominal cavity on day 2. In a negative control group, PBS was injected into both the tumor mass and peritoneal cavity. Each group contained five mice, and the representative result from three independent experiments is shown

HeLa cells, but not in NHDF. The discrepancy of CDDP sensitivity by Rad51 siRNA between NHDF and HeLa cells may be due to the difference of the CDDP uptake by the two cell lines. Indeed, the equitoxic dose of CDDP in NHDF and HeLa cells was 1.2 and 0.5 μg/ml, respectively, in our case (M. Ito and Y. Kaneda, unpublished data). Another possibility is that cell cycle difference between both cells may affect the sensitivity to CDDP in the presence of Rad51 siRNA. The precise mechanism of this different sensitivity to CDDP remains to be solved.

However, in human gene therapy, we should be very careful regarding the toxicity of Rad51 siRNA. As shown in Figure 5B, Rad51 siRNA alone induced apoptosis in both HeLa cells and NHDF, although the apoptotic cell ratio was much lower in the absence of CDDP. This may be consistent with the fact that Rad51 knockout mice are embryonic lethal [42]. To minimize the adverse effects to normal tissues, tumor-selective targeting is indispensable for cancer treatment. There are two ways to achieve selective targeting. One is the insertion of tumor-specific molecules to vectors, and another is the modification of vector size and charge. We have already reported that HVJ-cationic liposomes targeted tumor nodules in mouse peritoneum by intraperitoneal injection [43]. We are now constructing targeting vectors by modifying the HVJ envelope vector with polymers or tumor-specific single-chain antibodies.

When delivered by tumor-targeting vectors, siRNAs against genes resistant to cancer therapy hold great promise to become very effective anti-neoplastic therapeutics in combination with chemotherapy or radiotherapy.

Acknowledgements

We thank Atsuko Okuno and Konomi Higashidani for their excellent technical assistance. This work was supported by grant 15300163 for Y.K. from the Ministry of Education, Culture, Sports, Science and Technology of Japan.

References

1. Baird RD, Kaye SB. Drug resistance reversal – are we getting closer? *Eur J Cancer* 2003; **39**: 2450–2461.
2. Links M, Brown R. Clinical relevance of the molecular mechanisms of resistance to anti-cancer drugs. *Expert Rev Mol Med* 1999; **Oct 25**: 1–21.
3. Fojo T, Bates S. Strategies for reversing drug resistance. *Oncogene* 1988; **22**: 7512–7523.
4. Holleran WM, DeGregorio MW. Evolution of high-dose cisplatin. *Invest New Drugs* 1988; **6**: 135–142.
5. Weiss RB, Christian MC. New cisplatin analogues in development. *Drugs* 1993; **46**: 360–377.
6. Silvani A, Eoli M, Salmaggi A, *et al.* Phase II trial of cisplatin plus temozolomide in recurrent and progressive malignant glioma patients. *J Neurooncol* 2003; **66**: 203–208.
7. Roberts JJ, Kotsaki-Kovatsi VP. Potentiation of sulphur mustard or cisplatin-induced toxicity by caffeine in Chinese hamster cells correlates with formation of DNA double-strand breaks during replication on a damaged template. *Mutat Res* 1986; **165**: 207–220.
8. Kanno S, Hyodo M, Suzuki K, Ohkido M. Effect of DNA-damaging agents on DNA replication and cell-cycle progression of cultured mouse mammary carcinoma cells. *Jpn J Cancer Res* 1985; **76**: 289–296.
9. Zdraveski ZZ, Mello JA, Marinus MG, Essigmann JM. Multiple pathways of recombination define cellular responses to cisplatin. *Chem Biol* 2000; **7**: 39–50.
10. Xu Z, Chen ZP, Malapesta A, *et al.* DNA repair protein level vis-à-vis anticancer drug resistance in the human tumor cell

lines of the National Cancer Institute drug screening program. *Anticancer Drugs* 2002; **13**: 511–519.
11. D'Andrea AD, Grompe M. The Fanconi anemia/BRCA pathway. *Nat Rev Cancer* 2003; **3**: 23–34.
12. Sherr CJ. Principles of tumor suppression. *Cell* 2004; **116**: 235–246.
13. Henning W, Sturzbecher H-W. Homologous recombination and cell cycle checkpoints: Rad51 in tumor progression and therapy resistance. *Toxicology* 2003; **193**: 91–109.
14. Huang J, Dynan WS. Reconstitution of the mammalian DNA double-strand break end-joining reveals a requirement for an Mre11/Rad50/NBS1-containing fraction. *Nucleic Acids Res* 2002; **30**: 667–674.
15. Freit P, Canitrot Y, Muller C, *et al.* Cross-resistance to ionizing radiation in a murine leukemic cell line resistant cis-dichlorodiammineplatinum(II): role of Ku autoantigen. *Mol Pharmacol* 1999; **56**: 141–146.
16. Myint WK, Ng C, Raaphorst GP. Examining the non-homologous repair process following cisplatin and radiation treatments. *Int J Radiat Biol* 2002; **78**: 417–424.
17. Britten RA, Kuny S, Perdue S. Modification of non-conservative double-strand break (DSB) rejoining activity after the induction of cisplatin resistance in human tumour cells. *Br J Cancer* 1999; **79**: 843–849.
18. Omori S, Takiguchi Y, Suda A, *et al.* Suppression of a DNA double-strand break repair gene, Ku70, increases radio- and chemosensitivity in a human lung carcinoma cell line. *DNA Repair* 2002; **29**: 299–310.
19. Husain A, He G, Venkatraman ES, Spriggs DR. BRCA1 up-regulation is associated with repair-mediated resistance to cis-diamminedichloroplatinum(II). *Cancer Res* 1998; **58**: 1120–1123.
20. Aloyz R, Xu ZY, Bello V, *et al.* Regulation of cisplatin resistance and homologous recombinational repair by the TFIIH subunit XPD. *Cancer Res* 2002; **62**: 5457–5462.
21. Bhattacharyya A, Ear US, Koller BH, Weichselbaum RR, Bishop DK. The breast cancer susceptibility gene BRCA1 is required for subnuclear assembly of Rad51 and survival following treatment with the DNA cross-linking agent cisplatin. *J Biol Chem* 2000; **275**: 23 899–23 903.
22. Raderschall E, Stout K, Freier S, Suckow V, Schweiger S, Haaf T. Elevated levels of Rad51 recombination protein in tumor cells. *Cancer Res* 2002; **62**: 219–225.
23. Tijsterman M, Plasterk RH. Dicers at RISC; the mechanism of RNAi. *Cell* 2004; **117**: 1–3.
24. Dorsett Y, Tuschl T. siRNAs: applications in functional genomics and potential as therapeutics. *Nat Rev Drug Discov* 2004; **3**: 318–329.
25. Miyagishi M, Hayashi M, Taira K. Comparison of the suppressive effects of antisense oligonucleotides and siRNAs directed against the same targets in mammalian cells. *Antisense Nucleic Acid Drug Dev* 2003; **13**: 1–7.
26. Yokota T, Miyagishi M, Hino T, *et al.* siRNA-based inhibition specific for mutant SOD1 with single nucleotide alternation in familial ALS, compared with ribozyme and DNA enzyme. *Biochem Biophys Res Commun* 2004; **314**: 283–291.
27. Sioud M. Ribozyme- and siRNA-mediated mRNA degradation: a general introduction. *Methods Mol Biol* 2004; **252**: 1–8.
28. Kaneda Y, Nakajima T, Nishikawa T, *et al.* HVJ (hemagglutinating virus of Japan) envelope vector as a versatile gene delivery system. *Mol Ther* 2002; **6**: 219–226.
29. Oshima K, Shimamura M, Mizuno S, *et al.* Intrathecal injection of HVJ-E containing HGF gene to cerebrospinal fluid can prevent and ameliorate hearing impairment in rats. *FASEB J* 2004; **18**: 212–214.
30. Itoh Y, Kawamata Y, Harada M, *et al.* Free fatty acids regulate insulin secretion from pancreatic beta cells through GPR40. *Nature* 2003; **422**: 173–176.
31. Ahn J-D, Morishita R, Kaneda Y, *et al.* Inhibitory effects of novel AP-1 decoy oligodeoxynucleotides on vascular smooth muscle cell proliferation in vitro and neointimal formation in vivo. *Circ Res* 2002; **90**: 1325–1332.
32. Collis SJ, Swartz MJ, Nelson WG, DeWeese TL. Enhanced radiation and chemotherapy-mediated cell killing of human cancer cells by small inhibitory RNA silencing of DNA repair factors. *Cancer Res* 2003; **63**: 1550–1554.
33. Belenkov AL, Paiement J-P, Panasci LC, Monia BP, Chow TYK. An antisense oligonucleotide targeted to human Ku86 messenger RNA sensitizes M059 malignant glioma cells to ionizing radiation, bleomycin, and etoposide but not DNA cross-linking agents. *Cancer Res* 2002; **62**: 5888–5896.
34. Peng Y, Zhang Q, Nagasawa H, Okayasu R, Liber HL, Bedford JS. Silencing expression of the catalytic subunit of DNA-dependent protein kinase by small interfering RNA sensitizes human cells for radiation-induced chromosome damage, cell killing, and mutation. *Cancer Res* 2002; **62**: 6400–6404.
35. Jensen R, Glazer P. Cell-interdependent cisplatin killing by Ku/DNA-dependent protein kinase signaling transduced through gap junctions. *Proc Natl Acad Sci U S A* 2004; **101**: 6134–6139.
36. Durant S, Karran P. Vanillins – a novel family of DNA-PK inhibitors. *Nucleic Acids Res* 2003; **31**: 5501–5512.
37. Ohnishi T, Taki T, Hiraga S, Arita N, Morita T. In vitro and in vivo potentiation of radiosensitivity of malignant gliomas by antisense inhibition of the Rad51 gene. *Biochem Biophys Res Commun* 1998; **245**: 319–324.
38. Liu CM, Liu DP, Dong WJ, Liang CC. Retrovirus vector-mediated stable gene silencing in human cell. *Biochem Biophys Res Commun* 2004; **313**: 716–720.
39. Abbas-Terki T, Blanco-Bose W, Deglon N, Pralong W, Aebischer P. Lentiviral-mediated RNA interference. *Hum Gene Ther* 2002; **13**: 2197–2201.
40. Russell JS, Brady K, Burgan WE, *et al.* Gleevec-mediated inhibition of Rad51 expression and enhancement of tumor cell radiosensitivity. *Cancer Res* 2003; **63**: 7377–7383.
41. Hansen LT, Lundin C, Spang-Thomsen M, Peterson LN, Helleday T. The role of Rad51 in etoposide (VP16) resistance in small cell lung cancer. *Int J Cancer* 2003; **105**: 472–479.
42. Lim DS, Hasty P. A mutation in mouse rad51 results in an early embryonic lethal that is suppressed by a mutation in p53. *Mol Cell Biol* 1996; **16**: 7133–7143.
43. Miyata T, Yamamoto S, Sakamoto K, Morishita R, Kaneda Y. Novel immunotherapy for peritoneal dissemination of murine colon cancer with macrophage inflammatory protein-1β mediated by a tumor-specific vector, HVJ-cationic liposomes. *Cancer Gene Ther* 2001; **8**: 852–860.

J. Biomater. Sci. Polymer Edn, Vol. 16, No. 11, pp. 1447–1461 (2005)

Also available online - www.vsppub.com

Preparation of poly(ethylene glycol)-introduced cationized gelatin as a non-viral gene carrier

TOSHIHIRO KUSHIBIKI and YASUHIKO TABATA *

Department of Biomaterials, Institute for Frontier Medical Sciences, Kyoto University, 53 Kawara-cho Shogoin, Sakyo-ku, Kyoto 606-8507, Japan

Received 22 October 2004; accepted 16 April 2005

Abstract—The objective of this study was to prepare cationized gelatins grafted with poly(ethylene glycol) (PEG) (PEG-cationized gelatin) and evaluate the *in vivo* efficiency as a non-viral gene carrier. Cationized gelatin was prepared by chemical introduction of ethylenediamine to the carboxyl groups of gelatin. PEG with one terminal of active ester group was coupled to the amino groups of cationized gelatin to prepare PEG-cationized gelatins. Electrophoretic experiments revealed that the PEG-cationized gelatin with low PEGylation degrees was complexed with a plasmid DNA of luciferase, in remarked contrast to that with high PEGylation degrees. When the plasmid DNA complexed with the cationized gelatin or PEG-cationized gelatin was mixed with deoxyribonuclease I (DNase I) in solution to evaluate the resistance to enzymatic degradation, stronger protection effect of the PEG-cationized gelatin was observed than that of the cationized gelatin. The complex of plasmid DNA and PEG-cationized gelatin had an apparent molecular size of about 300 nm and almost zero surface charge. These findings indicate that the PEG-cationized gelatin–plasmid DNA complex has a nano-order structure where the plasmid DNA is covered with PEG molecules. When the PEG-cationized gelatin–plasmid DNA complex was intramuscularly injected, the level of gene expression was significantly increased compared with the injection of plasmid DNA solution. It is concluded that the PEG-cationized gelatin was a promising non-viral gene carrier to enhance gene expression *in vivo*.

Key words: Poly(ethylene glycol); gelatin; complex; gene delivery.

INTRODUCTION

The recent rapid development of molecular biology together with the steady progress of animal and plant genome projects has brought about some essential and revolutionary information on genes to elucidate all the biological phenomena at the molecular level [1–4]. In this situation, gene transfection is a key technology, indispensable to progress in molecular biology research [5–11]. Based on the

*To whom correspondence should be addressed. Tel.: (81-75) 751-4121. Fax: (81-75) 751-4646. E-mail: yasuhiko@frontier.kyoto-u.ac.jp

advent of genomics, new genes have been discovered and it is expected that they become therapeutically available for various diseases in near future. In this connection, gene therapy will be one of the new and promising medical therapies [12–16]. From the viewpoint of pharmaceutical sciences, it is necessary for successful gene therapy to achieve the delivery of genes to the target organ and tissue [17–20]. The objective of gene therapy is to allow a gene to express the coded protein in the target cells and consequently to treat disease by the protein secreted from transfected cells. Thus, it is important to develop a technology and methodology of a drug-delivery system to enhance the level of protein expression accompanied with gene transfection. For gene therapy, the viral gene carriers, such as adenovirus, retrovirus and adeno-associated virus, have been mainly used because of the high efficiency of gene transfection, although the clinical trials are quite limited by the adverse effects of virus itself, such as immunogenicity and toxicity or the possible mutagenesis of transfected cells. The new viral gene carrier with less adverse effects has been explored [21, 22], while the non-viral gene carrier has been investigated to enhance the transfection efficiency [6]. Comparable to the research and development of gene carriers, it will be important for *in vivo* gene therapy to control the body distribution of gene carriers and consequently that of gene complexed. When the complex of a plasmid DNA with a non-viral gene carrier is given to cells or injected into the body in the solution form, the plasmid DNA is rapidly and readily degraded and inactivated by enzymes or cells. As one practically possible way to minimize the enzymatic degradation of plasmid DNA, the surface of the plasmid DNA complex can be modified with polyethylene glycol (PEG) or PEG-like polymers. PEG has been chemically introduced to gelatin to prepare a PEG-introduced gelatin [23]. Following intravenous injection, the PEG-introduced gelatin was retained in the blood circulation for a longer time period than the original gelatin [23]. It is likely that gelatin is covered with PEG molecules and protected from the enzymatic attack and the exclusion by the reticuloendotherial system (RES).

Several synthetic materials, including cationic liposomes [24–26], poly(L-lysine) [27–30] and polyethylenimine [31–36], have been molecularly designed to demonstrate the successful DNA transfection into mammalian cells both *in vitro* and *in vivo*. Generally, since the plasmid DNA is a large and negatively charged molecule, it is impossible to allow the plasmid DNA to internalize into cells even though the attachment onto the cell membrane of negative charges takes place. When the plasmid DNA is polyionically complexed with synthetic cationic polymers, the molecular size of plasmid DNA decreases due to molecular condensation [37, 38]. It is likely that the condensed plasmid DNA–polymer complex of a positive charge can electrostatically interact with the cell membrane for internalization. Among the cationic polymers, it is known that the protonable amine residues of polyethylenimine could function as an endosomal buffering system which suppresses the action of endosomal enzymes to protect the plasmid DNA from degradation, the so-called buffering effect, resulting in the enhanced transfection efficiency [39].

Gelatin has been extensively used for industrial, pharmaceutical and medical applications. Its bio-safety has been proven through its long clinical usage as surgical biomaterial and drug ingredient. Another unique advantage is the electrical nature of gelatin which can be readily changed by the processing method of collagen for preparation [40]. For example, an alkaline processing allows collagen to structurally denature and hydrolyze the side chain of glutamine and asparagine residue. This results in generation of 'acidic' gelatin with an isoelectric point (IEP) of 5.0. On the other hand, an acidic processing of collagen produces 'basic' gelatin with an IEP of 9.0. We have prepared hydrogels by cross-linking gelatin for the controlled release of growth factors. Growth factors with IEP higher than 7.0, such as basic fibroblast growth factor [41], bone morphogenetic protein-2 [42], transforming growth factor beta1 [43] and hepatocyte growth factor [44], are immobilized into the biodegradable hydrogels of 'acidic' gelatin on the basis of the electrostatic interaction force between the growth factor and gelatin molecules. In this release system, the growth factor immobilized is not released from the gelatin hydrogel, unless the hydrogel carrier is degraded to generate water-soluble gelatin fragments. The growth factor release could be controlled only by changing the hydrogel degradation [41]. Depending on the nature of growth factors to be released, we can achieve their controlled release only if a biodegradable hydrogel is prepared from gelatin or the derivative which can physicochemically interact with the growth factor molecule. Another advantage of gelatin is to enable the chemical introduction with ease. For example, the cationized gelatin of positive charge can readily be prepared by introducing amine residues to the carboxyl groups of gelatin. The plasmid DNA polyionically immobilized in the cationized gelatin hydrogel is released from the hydrogel only if the hydrogel is degraded to generate the water-soluble degraded gelatin fragments [45, 46].

This study has been undertaken to evaluate the feasibility of a PEG-introduced cationized gelatin as a non-viral gene carrier. It is expected that PEG introduction (PEGylation) improves the biological stability of plasmid DNA against enzymatic attack, resulting in enhanced transfection efficiency *in vivo*.

MATERIALS AND METHODS

Materials

The gelatin sample with an IEP of 9.0 (MW = 10^5), prepared by an acid process of porcine skin, was kindly supplied by Nitta Gelatin (Osaka, Japan). 1-Ethyl-3-(3-dimethylaminopropyl) carbodiimide hydrochloride salt (EDC), β-alanine and 2,4,6-trinitrobenzensulfonic acid (TNBS) were purchased from Nacalai Tesque (Kyoto, Japan). Ethylenediamine was obtained from Wako (Osaka, Japan). Succinimidyl succinate-methoxy PEG (MW = 5000) was kindly provided by NOF (Tokyo, Japan).

Preparation of cationized gelatin

The carboxyl groups of gelatin were chemically modified by introducing amino groups for the cationization of gelatin [45, 46]. Both ethylenediamine and EDC were added at the molar ratio to the carboxyl groups of gelatin of 50 into 250 ml 100 mM phosphate-buffered solution (PBS, pH 7.4) containing 5 g of gelatin. Immediately thereafter, the solution pH was adjusted to 5.0 by adding 5 M HCl aqueous solution. The reaction mixture was agitated at 37°C for 18 h and then the reaction mixture was dialyzed in a cellulose tube (cut-off molecular weight $(12 - 14) \times 10^3$, Viskase, Willowbrook, IL, USA) against double-distilled water (DDW) for 48 h at room temperature and freeze-dried to obtain a cationized gelatin. When determined by the conventional TNBS method [47], the percentage of amino groups introduced into gelatin was 50.9 mol% of the carboxyl groups of gelatin.

PEG grafting of cationized gelatin

Cationized gelatin (1.0 μmol) was dissolved in anhydrous dimethylsulfoxide (DMSO, 10 g) at room temperature. Various amounts of succinimidyl succinate-methoxy PEG with (MW 5000; 0.1, 0.2, 1.0, 2.0 and 4.0×10^{-5} mol) were dissolved in 10 g DMSO and the solution was slowly added to the gelatin solution, followed by 3 h stirring at room temperature for PEGylation [23]. The reaction mixture was dialyzed in a cellulose tube (cut-off molecular weight $(12 - 14) \times 10^3$, Viskase) against DDW for 48 h at room temperature and freeze-dried to obtain a PEG-cationized gelatin. The PEGylation degree to the amino groups of cationized gelatin was determined by the conventional TNBS method [47].

Preparation of luciferase plasmid DNA

The pGL3 vector (5.26 kb) coding for the firefly luciferase gene (No. E1741, Luciferase Reporter Vectors-pGL3, Promega, Madison, WI, USA) was propagated in *Escherichia coli* (strain DH5α) and purified by column chromatography with the Qiagen EndoFree™ plasmid kit (No. 12362, Qiagen, Valencia, CA, USA) according to the manufacturers instructions. Yield and purity of the plasmid were ascertained by UV spectroscopy ($E_{260\,nm}/E_{280\,nm}$ ratio 1.8–1.9).

Preparation of PEG-cationized gelatin complexed with plasmid DNA

Complexation of PEG-cationized gelatin with luciferase plasmid DNA was performed by simply mixing the two materials at various N/P ratios (the number ratio of amino groups of gelatin to phosphate groups of DNA) in aqueous solution. Briefly, 50 μl PBS (pH 7.4) containing 2.5, 5, 10, 25, 50 and 100 μg of PEG-cationized gelatin was slowly added to the same volume of PBS containing 10 μg luciferase plasmid DNA at N/P ratios of 0.05, 0.1, 0.2, 0.5, 1.0 and 2.0. The mixed solution was gently agitated at 37°C for 30 min to form PEG-cationized gelatin–plasmid DNA complexes.

Light scattering measurement

To investigate the hydrodynamic radius of PEG-cationized gelatin plasmid DNA complexes, dynamic light scattering (DLS) measurement was carried out on a DLS 700 (Otsuka Electronics, Osaka, Japan) equipped with He-Ne^- laser at a detection angle of 90° at room temperature. The cationized gelatin and PEG-cationized gelatin plasmid DNA complexes were prepared in PBS at 37°C with 5 mg/ml of respective cationized gelatin solution at a N/P ratio of 1. The hydrodynamic diameter of cationized gelatin and PEG-cationized gelatin complexed with plasmid DNA was analyzed based on the cumulants method and automatically calculated by the computer software equipped to express as the apparent molecular size. Electrophoretic light scattering (ELS) measurement was carried on an ELS-7000 (Otsuka Electronics) at room temperature and an electric field strength of 100 V/cm. The complex samples were prepared similarly other than using 10 mM phosphate buffer (pH 7.4). The zeta potential was automatically calculated using the Schmoluchowski equation. Each experiment was done 10–20 times independently, unless stated otherwise.

Nuclease resistance of plasmid DNA complexed with PEG-cationized gelatin

Nuclease resistance of plasmid DNA with or without PEG-cationized gelatin complexation was evaluated by the method reported by Katayose and Kataoka [49]. In brief, PBS containing 10 mM $MgCl_2$ was added either to a solution (2 ml) of the cationized gelatin or PEG-cationized gelatin complex with 20 μg plasmid DNA at a N/P ratio of 1.0. DNase I from bovine pancreas (100 units, #D4527, Sigma, St. Louis, MO, USA) was added to each sample and the time profile of optical density was recorded at 260 nm at 25°C for 30 min. After that, every sample was subjected to a gel retardation assay to estimate plasmid DNA degradation.

Electrophoresis of PEG-cationized gelatin–plasmid DNA complexes

Formation of PEG-cationized gelatin–plasmid DNA complexes was confirmed by the gel retardation assay [48]. An aliquot (5 μl) of plasmid DNA complex solution (0.1 μg/μl) was loaded into a well of an ethidium bromide gel containing 0.8% agarose and electrophoresed at 100 V for 15 min in Tris-borate-EDTA (TBE) buffer. Bands corresponding to plasmid DNA were detected under UV light and photographed.

In vivo *assessment of gene expression following injection of PEG-cationized gelatin–plasmid DNA complexes*

The complex of plasmid DNA and cationized gelatin or PEG-cationized gelatins prepared at different mixing N/P ratios were injected into the left femoral muscle of ddY mice (6–7 weeks old, Nihon SLC, Shizuoka, Japan). The dose of plasmid DNA was 100 μg/100 μl PBS (pH 7.4) per mouse. The mouse muscle was taken out

1, 3, 7 and 14 days after injection. All the animal experiments were done according to the Institutional Guidance of Kyoto University on animal experimentation. Luciferase gene expression was measured by luminescence. The mouse muscle was homogenized in 500 μl lysis buffer (No. E1531, Lysis Reagent, Promega) using a Polytron homogenizer (No. PT-MR 3100, Kinematica, Littau, Switzerland). The sample lysate (300 μl) was transferred to a centrifuge tube, followed by a freeze-and-thaw process 3 times. The lysate was centrifuged at $14 \times 10^3 \times g$ for 10 min at 4°C and 250 μl of supernatant sample was mixed with 50 μl of a reconstituted luciferase assay solution (No. E2610, Luciferase Assay System, Promega) and the relative light unit (RLU) of the solution mixture was determined by a luminometer (MicroLumatPlus LB 96V, Berthold, Tokyo, Japan). The total protein of each supernatant was determined by BCA Protein Assay Reagent (Pierce, Rockford, IL, USA) in order to normalize the influence of weight variance of mouse muscle on the luciferase activity. Each experiment group consisted of three mice.

Statistical analysis

All the data were expressed as the mean±standard derivation of the mean. Statistical significance (defined as $P < 0.01$) was evaluated based on the unpaired Student's t-test (two-tailed).

RESULTS

Preparation of PEG-introduced cationized gelatin

Figure 1 shows the percentage of PEG introduced (PEGylation degree) to the amino groups of cationized gelatin as a function of that of PEG added. The number of amino groups of cationized gelatin was 75 (mol/mol gelatin) [45, 46]. PEG was successfully introduced into the cationized gelatin, while non-reacted PEG

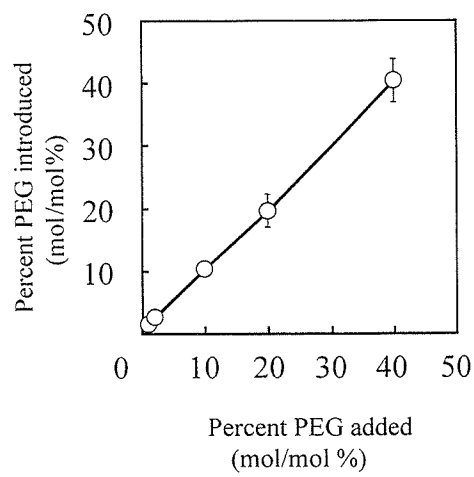

Figure 1. The percentage of PEG introduced to the amino groups of cationized gelatin as a function of that of PEG added for grafting reaction.

was completely removed by dialysis. No PEG remained, as confirmed by gel-permeation chromatography (data not shown). The PEGylation degrees were 1.1, 2.1, 10, 20 and 40 (mol/mol%) when PEG was added initially at 1, 2, 10, 20 and 40 (mol/mol%). The PEGylation degree could be controlled by changing the amount of PEG added.

Characterization of PEG-introduced cationized gelatin and the complex with plasmid DNA

Figure 2 shows the electrophoretic patterns of cationized gelatin or PEG-cationized gelatin–plasmid DNA complexes prepared at different mixing N/P ratios. The band of plasmid DNA was not migrated when the PEGylation degree of PEG-cationized gelatin used was 0 or 1.1 at N/P ratios of 0.5 or higher. A similar result was observed when the PEGylation degree of PEG-cationized gelatin was 2.1 or 10 at the N/P ratio of 2.0. However, the plasmid DNA band had migrated similar to the original plasmid DNA at PEGylation degrees of 20 and 40.

Figure 3 summarizes the apparent molecular size of plasmid DNA complexed with various PEG-cationized gelatins at different mixing N/P ratios. The apparent molecular size of complexes decreased with an increase of N/P ratio when the PEGylation degree of PEG-cationized gelatin was 0 [50], 1.1 or 2.1. However, no significant difference in the apparent molecular size was observed, irrespective of the N/P ratio for the PEG-cationized gelatin with PEGylation degrees of 10, 20 and 40. The zeta potential of PEG-cationized gelatin–plasmid DNA complexes tended to increase with increasing N/P ratio when the PEGylation degree of cationized gelatin was 1.1 and 2.1 (Fig. 4). In contrast, this tendency was not observed when the PEGylation degree was 10, 20 or 40. However, there was no significant difference in the zeta potential between the complexes at different mixing N/P ratios.

Figure 5a shows the time-course of UV absorbance of plasmid DNA or that complexed with the cationized gelatin or PEG-cationized gelatin after enzyme treatment. This is a test to evaluate the resistance of plasmid DNA against nuclease hydrolysis; an increase in the absorbance indicates the high susceptibility to enzymatic degradation of plasmid DNA. For the free plasmid DNA, absorbance of the solution rapidly increased with time due to the fragmentation of the DNA. However, no substantial increase in absorbance was observed for plasmid DNA complexed with PEG-cationized gelatin with the PEGylation degree of 10 or lower. On the other hand, when the PEGylation degree was 20 or higher, or 0, the absorbance again increased. Figure 5b shows the electrophoretic pattern of plasmid DNA complexed with the PEG-cationized gelatin at different PEGylation degrees after DNase I treatment. When the plasmid DNA was complexed with the PEG-cationized gelatin at the PEGylation degree of 10 or lower, the band of plasmid DNA was not migrated after the DNase I treatment. However, when the PEGylation degree was 20 or higher, or 0, the band migration was observed.

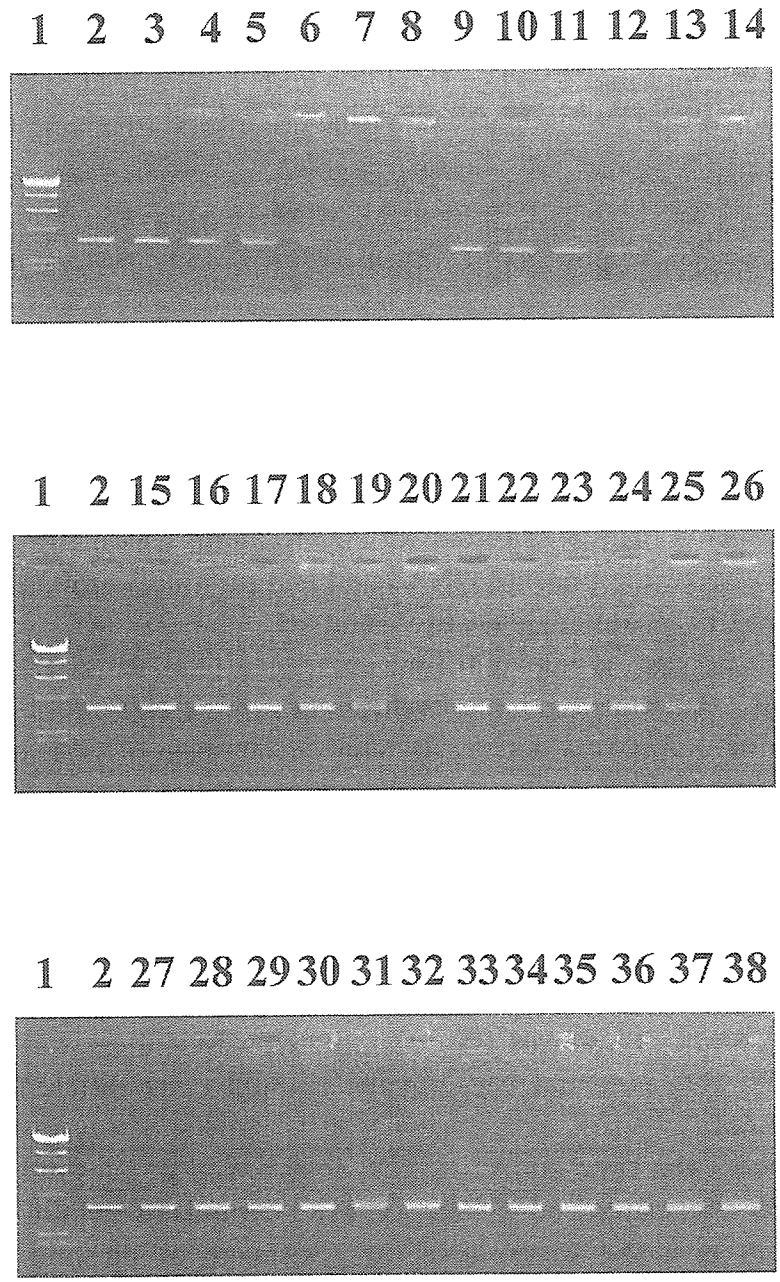

Figure 2. Electrophoretic patterns of cationized gelatin or PEG-cationized gelatin–plasmid DNA complex prepared at different N/P mixing ratios. Lane 1, molecular marker; lane 2, naked plasmid DNA. Lanes 3–8, plasmid DNA complexed with cationized gelatin at N/P ratios of 0.05, 0.1, 0.2, 0.5, 1.0 and 2.0, respectively. Lanes 9–14, plasmid DNA complexed with PEG-cationized gelatin with a PEGylation degree of 1.1 at N/P ratios of 0.05, 0.1, 0.2, 0.5, 1.0 and 2.0, respectively. Lanes 15–20, plasmid DNA complexed with PEG-cationized gelatin with a PEGylation degree of 2.1 at N/P ratios of 0.05, 0.1, 0.2, 0.5, 1.0 and 2.0, respectively. Lanes 21–26, plasmid DNA complexed with PEG-cationized gelatin with a PEGylation degree of 10 at N/P ratios of 0.05, 0.1, 0.2, 0.5, 1.0 and 2.0, respectively. Lanes 27–32, plasmid DNA complexed with PEG-cationized gelatin with a PEGylation degree of 20 at N/P ratios of 0.05, 0.1, 0.2, 0.5, 1.0 and 2.0, respectively. Lanes 33–38, plasmid DNA complexed with PEG-cationized gelatin with a PEGylation degree of 40 at N/P ratios of 0.05, 0.1, 0.2, 0.5, 1.0 and 2.0, respectively.

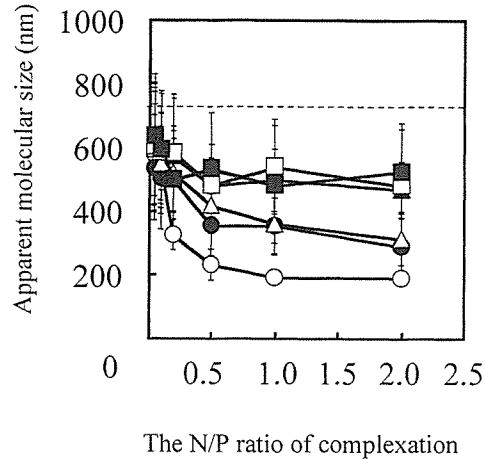

Figure 3. The apparent molecular size of plasmid DNA complexed with PEG-cationized gelatin with different PEGylation degrees at different mixing N/P ratios. The PEGylation degree of PEGgelatin used was 0 (○) (native cationized gelatin), 1.1 (●), 2.1 (△), 10 (▲), 20 (□) and 40 (■) mol/mol of cationized gelatin. A dotted line indicates the apparent molecular size of naked plasmid DNA.

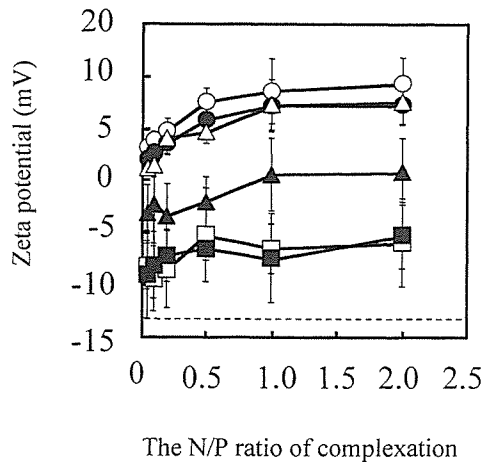

Figure 4. The zeta potential of plasmid DNA complexed with PEG-cationized gelatin with different PEGylation degrees at different mixing N/P ratios. The PEGylation degree of PEG-gelatin used was 0 (○) (native cationized gelatin), 1.1 (●), 2.1 (△), 10 (▲), 20 (□) and 40 (■) mol/mol cationized gelatin. A dotted line indicates the zeta potential of naked plasmid DNA.

In vivo *transfection efficiency of PEG-cationized gelatin–plasmid DNA complex*

Figure 6 shows the luciferase activity of mouse muscles after intramuscular injection of plasmid DNA complexed with the cationized gelatin or PEG-cationized gelatin at a PEGylation degree of 1.1 at various N/P ratios. This is because complexation with the PEG-cationized gelatin at this PEGylation degree gave the plasmid DNA from the DNase I degradation (Fig. 5). When the N/P ratio was 0.1, low luciferase activity was clearly observed for every group. However, at the N/P ratios of 0.5 or higher, the luciferase activity by the PEG-cationized gelatin increased and was significantly higher than that of other groups. Moreover, the luciferase activity after injection of PEG-cationized gelatin–plasmid DNA complexes tended

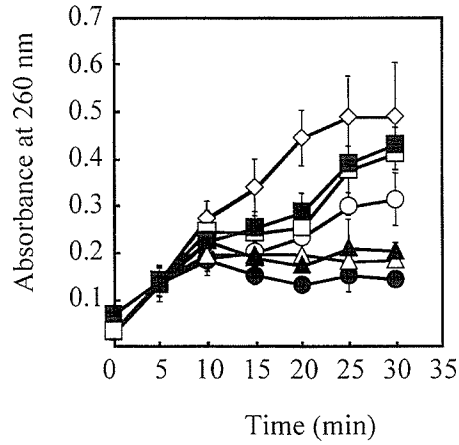

(a)

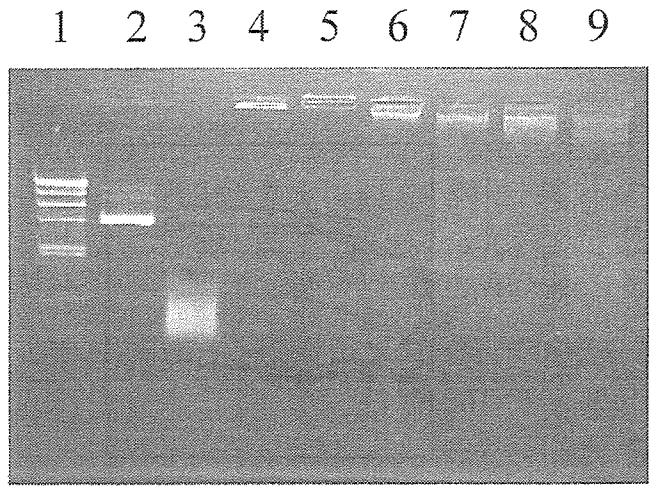

(b)

Figure 5. (a) DNase I degradation profile of plasmid DNA complexed with PEG-cationized gelatin with different PEGylation degrees. The PEGylation degree of PEG-gelatin used was 0 (○) (native cationized gelatin), 1.1 (●), 2.1 (△), 10 (▲), 20 (□) and 40 (■) mol/mol of cationized gelatin. The N/P ratio is 1.0. (◇) indicates the degradation profile of naked plasmid DNA by DNase I. (b) Electrophoretic patterns of plasmid DNA complexed with PEG-cationized gelatin with different PEGylation degrees after incubation with DNase I. Lane 1, molecular marker; lane 2, intact naked plasmid DNA; lane 3, degraded plasmid DNA. Lanes 4–8, plasmid DNA complexed with cationized gelatin at PEGylation degrees of 1.1, 2.1, 10, 20 and 40, respectively. Lane 9, plasmid DNA complexed with original cationized gelatin.

to increase significantly, in remarkable contrast to the cationized gelatin–plasmid DNA complex.

DISCUSSION

The present study clearly demonstrates that when the plasmid DNA was mixed to complex with the PEG-cationized gelatin, the DNase I digestion of plasmid DNA was suppressed and the *in vivo* transfection efficiency of plasmid DNA was in-

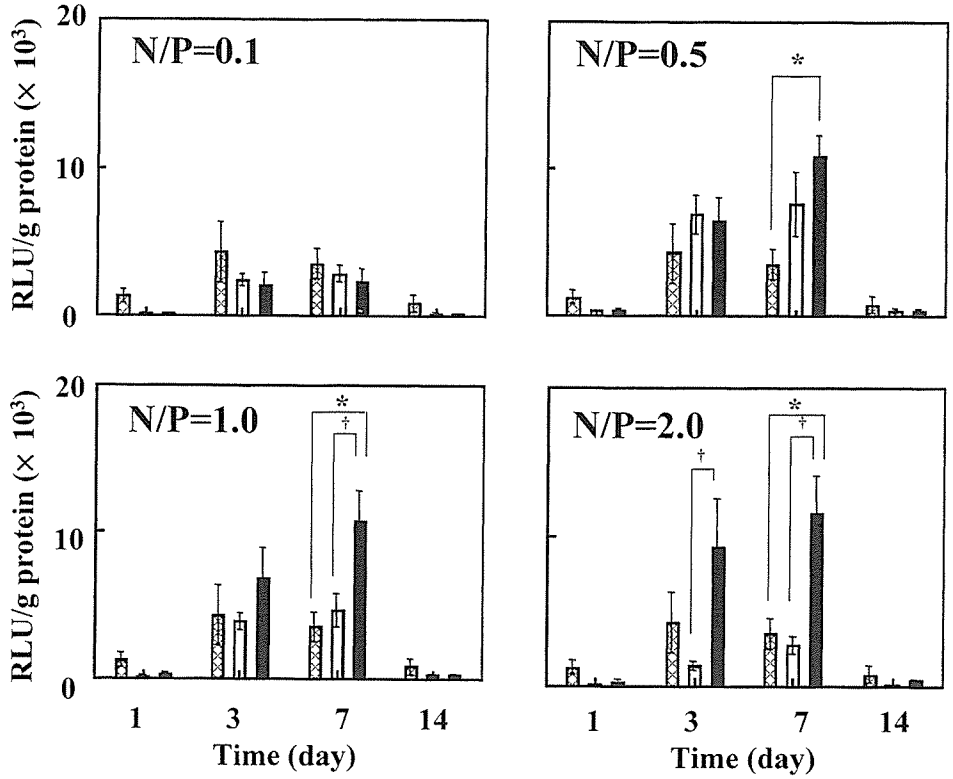

Figure 6. Luciferase activity of mouse muscles after intramuscular injection of cationized gelatin or PEG-cationized gelatin complexed with plasmid DNA at various N/P ratios. Plasmid DNA was complexed with original cationized gelatin (□) and PEG-cationized gelatin with a PEGylation degree of 1.1 (■). The cross-hatched bar indicates luciferase activity after injection of naked plasmid DNA. $^{*}P < 0.05$, significant against the RLU value of mice injected with original plasmid DNA; $^{\dagger}P < 0.05$, significant against the RLU value of mice injected with plasmid DNA complexed with cationized gelatin.

creased. In this study, the percentage of amino groups introduced into gelatin was 50.9 mol% of the carboxyl groups of gelatin because the cationization extent was high enough to give the lacZ plasmid DNA complex positive charge necessary for gene expression [47]. The gel retardation assay revealed that the PEG-cationized gelatin interacted electrostatically with the plasmid DNA. It is possible that the negative charge of plasmid DNA is neutralized by complexation with PEG-cationized gelatin and the molecular size of plasmid DNA is increased by complexation with the PEG-cationized gelatin, resulting in reduced electrophoretic migration of plasmid DNA. However, with a further increase in the PEGylation degree of cationized gelatin the amine residues of PEG-cationized gelatin were decreased by PEGylation, which allows the plasmid DNA to weaken the polyionic interaction with the PEG-cationized gelatin. In addition, it is likely that PEG grafting prevents the plasmid DNA to stereochemically approach the PEG-cationized gelatin, resulting in suppressed polyion complexation. This result indicates that the primary amine groups of PEG-cationized gelatin play an important role in the complexation with plasmid DNA. The PEG-cationized gelatin–plasmid DNA complex showed an apparent molecular size in the nanometer range (Fig. 3). The complex size was around

300 nm at PEG-ylation degrees of 1.1 and 2.1. It has been demonstrated that the complex with this size range can be favorably taken up by cells [51, 52]. This is also a merit of the plasmid–DNA complex prepared from the PEG-cationized gelatin for enhanced gene expression in terms of efficient DNA packing to nanosize particles. However, the apparent molecular size of complexes by PEG-cationized gelatin with PEGylation degrees of 10, 20 and 40 was not decreased. This is due to decrease in the primary amine group which can interact with the plasmid DNA. The surface charge of PEG-cationized gelatin–plasmid DNA complex was tended to increase with increasing N/P ratio when the PEGylation degree was 1.1 or 2.1 (Fig. 4). These findings strongly suggest that the PEG-cationized gelatin–plasmid DNA complex has a nano-size micellar structure of which the surface is covered with PEG molecules.

It is important for increasing transfection efficiency to inhibit the degradation of plasmid DNA by nuclease before transfection to cells. The effect of PEG-cationized gelatin on protection of plasmid DNA from DNase degradation was examined using DNase I as a model enzyme (Fig. 5). After incubated with DNase I at 25°C, the plasmid DNA complexed with PEG-cationized gelatin at PEGylation degrees of 20 and 40, as well as naked plasmid DNA was degraded with time, whereas the enzymatic degradation of plasmid DNA complexed with PEG-cationized gelatin at PEGylation degrees of 1.1 and 2.1 was suppressed. It is possible that PEG-cationized gelatin at the lower PEGylation degrees complexed the plasmid DNA more firmly than that at the higher PEGylation degrees, resulting in reduced DNase attack to the plasmid DNA. This is because the lower degree of PEGylation did not suppress the complexation between the plasmid DNA and PEG-cationized gelatin in terms of the remaining of amine contents and the lowering steric hindrance effect of PEG molecules. The PEG-cationized gelatin with higher PEGylation degrees cannot firmly form the complex with the plasmid DNA. As a result, the plasmid DNA would be readily attacked by the DNase to degrade. However, the presence of PEG molecules for the PEG-cationized gelatin–plasmid DNA complex will protect the plasmid DNA from the enzymatic attack, because of the 'stealth' effect of PEG [53, 54]. It is conceivable that this effect enables the plasmid DNA to suppress the enzymatic degradation, resulting in slightly reduced increase in the absorbance compared with free plasmid DNA. This finding suggests that in physiological conditions, where the nuclease concentration is markedly lower than the concentration tested, such complexation will significantly protect the plasmid DNA from the enzymatic degradation *in vivo*.

Kakizawa and Kataoka have reported delivery systems of genes and related compounds with PEG-based polymer micelles [57]. Block co-polymers, composed of cationic and hydrophilic segments, associate spontaneously with polyanionic DNAs to form their micelles. The research data revealed that the formation of PEG-based polymer micelles protects the plasmid DNA from DNase degradation. It should be noted that the surface of the micelles was not completely covered with PEG molecules because the polymer micelles showed a positive charge. These

findings demonstrate that it was not always necessary to completely cover the micelle with PEG chains to protect the plasmid DNA incorporated from DNase degradation. In this study, we prepared a PEG-cationized gelatin complex at the PEGylation degrees of 1.1 or 2.1, which has a slightly positive charge of the surface. Since it is necessary for the complexes to adhere and internalize into cells for transfection, the surface charge of the complex should be positive. Moreover, there is no doubt that the surface presence of PEG molecules is also required from the viewpoint of plasmid DNA protection from enzymatic attack. As expected, as the number of PEG molecules on the surface of the complex increased, the enzymatic degradation of plasmid DNA was suppressed. On the other hand, the positive surface charge is important to enhance the transfection efficiency. Thus, it is concluded that a balance of the surface charge of complexes and the protection efficiency from enzymatic attack was important for the transfection efficiency of PEG-introduced cationized gelatin–plasmid DNA complexes.

Generally, gelatin is not degraded by simple hydrolysis, but by proteolysis. Therefore, in this study, the transfection experiments of PEG-cationized gelatin–plasmid DNA complex have been carried out in the mouse muscle. The highest luciferase activity was obtained at 7 day post-administration of PEG-cationized gelatin–plasmid DNA complex, but the expression level of luciferase declined thereafter (Fig. 6). When the N/P ratio was 0.1, the luciferase activity was similar to that of plasmid DNA solution. This phenomenon is due to the absence of complex formation at this N/P ratio. In contrast, the luciferase activity was significantly higher than that of plasmid DNA solution and cationized gelatin–plasmid DNA complex at N/P ratios of is 0.5, 1.0 and 2.0. This can be explained in terms of the *in vivo* stability of plasmid DNA. It is highly possible that complexation with the PEG-cationized gelatin enables plasmid DNA to enhance the resistance against the enzymatic degradation, as well as the extent accumulated at the injected site, resulting in a higher level and longer time period of gene expression. LipofectAmine® (InVitrogen, Carlsbad, CA, USA), which has extensively been used as a transfection reagent, was used for a comparison study. The luciferase activity was 5×10^3 RLU/g protein, which was similar to that of the present complexes. Considering the transfection reagent used *in vitro* researches of biology and medicine, both LipofectAmine® and cationized polymers previously reported may be useful. However, there are many problems to be solved for the *in vivo* application, such as toxicity, the degradation of transgene by enzyme before transfection and the targetability to the site of action. It is known that hydrodynamic gene delivery, which involves the rapid intravascular injection of a large volume of DNA-containing fluid, is one of the effective transfection methods. In this method, a large volume of fluid is generally required for injection. However, in this study, the injection of large volume of solution was not done. It is likely that the large volume injection enables the plasmid DNA to enhance the level of gene expression, irrespective of the injected form.